Self-organisation of fullerene-containing conical supermesogens

Stavros D. Peroukidis, Alexandros G. Vanakaras* and Demetri J. Photinos

Received 20th September 2007, Accepted 20th November 2007
First published as an Advance Article on the web 11th January 2008
DOI: 10.1039/b714506c

A molecular model of cubic building blocks is used to describe the mesomorphism of conical fullerenomesogens. Calculations based on density functional molecular theory and on Monte Carlo computer simulations give qualitatively similar results that are also in good agreement with the experimentally observed mesomorphic behaviour. The columnar and lamellar mesophases obtained are non-polar, and their relative stability is controlled by a single model parameter representing the softness of the repulsive interactions among the building blocks of the conical molecules.

1. Introduction

Conventional columnar liquid crystals (LCs) are made of disc-like molecules. Typically, these molecules have a flat rigid core with peripherally attached flexible alkyl chains and they stack in columns which self-organise in phases of three-, four- or six-fold rotational symmetry about the column axis.[1] Following the discovery by Chandrasekhar *et al.*[2] in 1977 of what today is referred to as conventional low molar mass discotic mesophases, a variety of novel columnar LC systems have been identified. Their building blocks range from chiral molecules,[3] inverted molecules,[4] tapered molecules,[5] half disc molecules,[6–8] bowl-like[9] (pyramidic,[10] cone-shaped[11]) molecules, dendrimers[12] and fullerodendrimers,[13] symmetric-tapered molecules,[14,15] hybrid organic–inorganic polycatenar[16] or multipode supermesogens[17] and conical (badminton shuttlecock) multiadducts of C60.[18–20] From the applications point of view, the general interest in columnar LC phases[1] is based on the versatility they offer for the controllable self-assembly of molecular entities into one-dimensional arrays that can be ordered in the other two dimensions.

In columnar LCs formed by conical molecules, the stacking within the columns can be strongly biased by their steric molecular asymmetry. Accordingly, such LCs may exhibit physical properties characteristic of polar or inversion asymmetric media,[21] such as ferroelectricity, second harmonic generation, *etc*. In particular, the columnar mesomorphism in the case of conical molecules with a fullerene apex[18–20] appears to be driven by a simple mechanism: the hollow cones self-assemble into polar stacks, with the apex of each cone resting within the empty conical part of its neighbour. The polar columns in turn self-organise into LC columnar phases that, for all known systems, do not exhibit any macroscopic polarisation.

In this paper, motivated by the experimental observations[18–20,23] of stable LC columnar phases of fullerene multiadducts of conical shape, we study, by molecular theory and Monte Carlo (MC) molecular simulations, the phase behaviour and the molecular organisation of model fullerene-containing hollow cones. In the next section we introduce a general way of coarse-grain modelling of complex molecular architectures together with the statistical mechanical theoretical framework for the exploration of possible order–disorder phase transitions. In the same section we present and discuss the calculated phase behaviour and the corresponding molecular organisation of the model cone molecules. In section 3 we outline the MC computer experiments and we analyse the findings. The conclusions from the combined theory-simulation study are drawn in section 4.

Department of Materials Science, University of Patras, Patras, 26504, Greece. E-mail: a.g.vanakaras@upatras.gr

2. Molecular modelling and analytical calculations

To formulate the intermolecular potential we follow the block model approach that has been introduced recently[22] and has been applied successfully to the study of the liquid-crystalline polymorphism and the molecular organisation of a variety of fullerene-containing molecular architectures. In this coarse-grained representation, the dominant molecular shape (or shapes, in the case of flexible molecules) is built from a number of equal size cubic blocks of side length equal to the effective diameter of a fullerene molecule. To account for the submolecular partitioning into chemically distinct parts, different kinds of blocks are to be used. In the case of the conical molecules considered here (Fig. 1a) the molecular cone consists of $b_n = 25$ building blocks: one block corresponds to the fullerene unit (f-block) and 24 blocks build up the grafted addends (m-blocks) in the way shown in Fig. 1b. To simplify the calculations we assume that the overall coarse-grained molecular structure is restricted to translate and rotate in a cubic lattice. The lattice constant coincides with the size of the cubic blocks.

For the block–block interactions, it is assumed that two building blocks belonging to different molecules interact only upon simultaneous occupation of the same lattice site. The intermolecular interaction potential of molecules I and J is then the sum of block–block interactions,

$$U_{\mathrm{IJ}} = \sum_{b_{\mathrm{I}},b_{\mathrm{J}}} u_{b_{\mathrm{I}},b_{\mathrm{J}}}\delta(R_{b_{\mathrm{I}},b_{\mathrm{J}}}) \quad (1)$$

where the argument of the δ-function, $R_{b_{\mathrm{I}},b_{\mathrm{J}}}$, denotes the distance of blocks b_{I} and b_{J}, and $u_{b_{\mathrm{I}},b_{\mathrm{J}}}$ is the intermolecular potential of a pair of blocks; the block index, b, can be either f or m. For the calculations presented here we have chosen $u_{\mathrm{f,f}} = u_{\mathrm{f,m}} = \infty$ and $u_{\mathrm{m,m}} = u$, with u a positive parameter expressing the strength of the repulsive potential between two m-blocks. According to

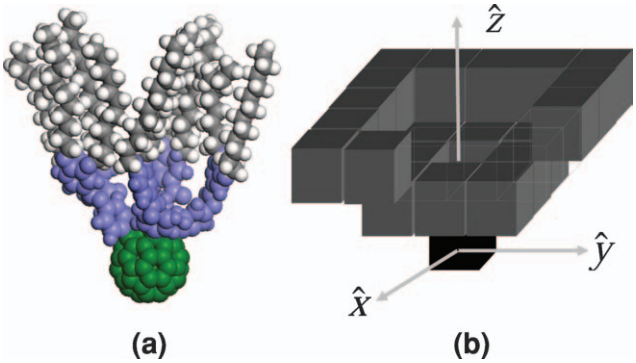

Fig. 1 (a) Space-filling representation of the chemical structure of a conical "badminton shuttlecock" molecule[19] consisting of a C60 fullerene apex and five aromatic groups attached around a pentagon of the fullerene. (b) Block representation of the same molecule. The black block corresponds to the fullerene unit and the light grey blocks to the addend groups. The molecular axes are also shown.

the above parameterisation, a fullerene, f, block is impenetrable by any block while two mesogenic, m, blocks can occupy the same space albeit at the expense of an increase in the interaction energy by u. It should be noted that certain strongly interdigitating molecular pair configurations yield vanishing values for the intermolecular potential in the particular block representation of eqn (1). Cross-sections of these configurations are shown in Fig. 2. Since such configurations are highly unlikely to occur in the real systems, they are completely suppressed in the calculations by assigning to them additional high values for the intermolecular potential. However, the inclusion of these configurations, with the intermolecular energy derived directly from eqn (1), does not change the final results appreciably.

In the geometry adopted for the present model, the grafted addends are assigned a length $l_g = 2\sqrt{2}l_0$, with l_0 denoting the size of the cubic blocks. Setting the latter equal to the fullerene diameter, $l_0 \approx 9$ Å, leads to $l_g \approx 25$ Å, which is a reasonable estimate for the fully extended conformations of the addends. However, the volume assigned collectively to the addends of a single molecule (24 out of the 25 blocks) cannot be considered as a hard-body excluded volume but rather as an effective volume that is accessible to them on account of their flexibility and the possible softness of their repulsive interactions. In other words, the purely steric total volume of the addends of a single molecule is less than 24 times the fullerene steric volume.

The analytical results for the phase behaviour and for the single-particle distribution function in the various phases are

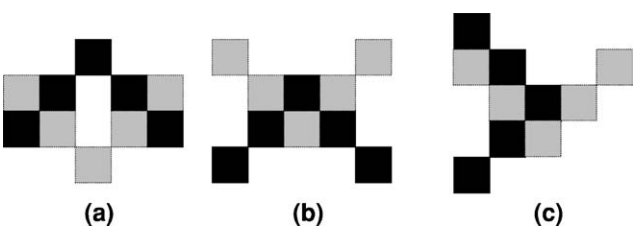

Fig. 2 Cross sections of interdigitating configurations of molecular pairs for which the block–additive interaction potential in eqn (1) vanishes. Gray and black tones are used to distinguish between blocks belonging to different molecules.

based on an approximate, Onsager-type, expression for the Helmholtz free-energy density functional[21,22] of the form

$$\begin{aligned} -FNk_BT \approx & \ln \int \mathrm{d}\varpi_I \zeta(\varpi_I) + \\ & + \tfrac{1}{2}(N-1)\ln \int d\varpi_I \int \mathrm{d}\varpi_J \rho(\varpi_I)\rho(\varpi_J) \\ & \times \exp(-U_{IJ}(\varpi_I, \varpi_J)/k_BT) \end{aligned} \quad (2)$$

Here, the collective variable $\varpi \equiv (R_I, \Omega_I)$ denotes the molecular position R_I and orientation Ω_I, $\zeta(\varpi_I)$ is the variational weight function of molecule I and $\rho(\varpi_I) = \zeta(\varpi_I)/\int \mathrm{d}\varpi_I \zeta(\varpi_I)$ is the single-molecule position-orientation distribution function. Due to the restriction of the rotations and translations to a cubic lattice, all the integrations in the above expressions reduce to summations over the lattice points.

Given the number density $\bar{\rho} = N/V$, (number N of particles over the volume V) and temperature T (or, equivalently the dimensionless parameter u/k_BT, with k_B denoting the Boltzmann constant) we calculate the single-particle distribution $\rho(\varpi_I)$ from the variational self-consistency equations imposed on the free-energy functional.[22] The symmetries of the sought solutions correspond to the isotropic, nematic, orthogonal smectic and columnar phases. Having obtained the single-particle distribution it is straightforward to calculate the free energy, the pressure and the chemical potential at any given density and temperature. Phase boundaries in the pressure–temperature and/or the density–temperature planes are then calculated from the coexistence conditions obtained by equating pressures and chemical potentials of the coexisting phases.

Introducing the dimensionless pressure p^* ($\equiv Pv_0/u$) where v_0 is the volume of a building block, we present in Fig. 3a and 3b the calculated transition pressures and the coexistence densities, respectively, as functions of $u^* \equiv u/k_BT$. The dimensionless parameter u^* can be read either as a measure of the addend m-block hardness (impenetrability) or as an inverse temperature of the system. All the phase transitions are found to be of first order, with the density jump at the columnar–isotropic phase transition being considerably larger than both the corresponding jump at the smectic to columnar transition and the very small density jump at the isotropic to smectic phase transition. Crystal phases are not explicitly included in the calculations, and therefore the columnar and smectic phases persisting in the high pressure (or density) ends of the calculated phase diagrams in Fig. 3 would in fact be pre-empted by respective crystal phases. It is also worth noting that the conical shape of the molecules becomes less restrictive to their packing as the values of the interaction parameter u^* decreases since, in that case, the energetic cost for the molecular addends to occupy the same space becomes small.

Regarding the relevant range of u^*, the phase diagrams in Fig. 3 suggest that systems for which a direct isotropic–columnar transition is observed experimentally[19,20] correspond to $u^* > 0.1$. On the other hand, as shown very recently by Zhong *et al.*,[23] a suitable chemical modification of the five addend branches and the insertion of a methyl group at the centre of the molecular cavity, retaining the overall molecular architecture, may lead to lamellar phases over a wide range of temperatures. Interestingly, this type of molecular organisation is predicted by the calculated phase diagram in Fig. 3, indicating that our simple model is capable of reproducing the experimentally observed lamellar organisation when $u^* < 0.1$. Viewing the interaction parameter u^* as a measure of the hardness of the conical periphery, it follows that

This journal is © The Royal Society of Chemistry 2008

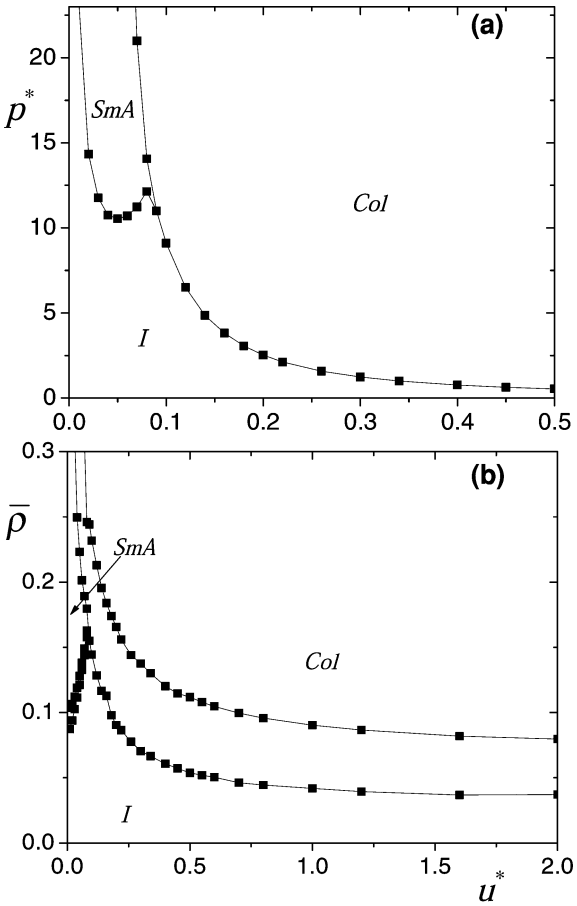

Fig. 3 Calculated phase diagrams using the free-energy functional of eqn (2). (a) Pressure and (b) coexistence densities at the transition *vs.* scaled inverse temperature u^*.

there is a critical hardness above which the lamellar molecular organisation is destabilised in favour of the columnar.

The calculated single-particle distribution function in the lamellar phase shows that the periodic layers are three blocks thick and apolar. This corresponds to a microsegregated structure where the molecules, packed with their cone axis normal to the layers, form successive fullerene-rich and mesogen-rich sublayers of thickness equal to one and two block-lengths, respectively. Clearly, this packing motif implies considerable overlapping of the volumes assigned to the mesogenic blocks of adjacent molecules, which explains why it is obtained only for small values of the "hardness" u^*.

The orientationally-averaged two-dimensional density profile of the fullerene units on a plane perpendicular to the columns is defined by $\rho_\perp(x, y) \equiv \int \mathrm{d}z \mathrm{d}\Omega \rho(\varpi)$. Representative profiles of $\rho_\perp$ are shown in Fig. 4 for $p^* = 5$ and $u^* = 0.3$. At these thermodynamic conditions, according to Fig. 3a, the system is well within the region of stability of the columnar phase. It is clear from this plot that the columns are organised in a two-dimensional orthogonal lattice with unit-cell lattice constants $d_x = d_y = 5$. Comparison of the unit-cell lengths with the molecular dimensions indicates that there is no appreciable inter-columnar lateral overlapping. Furthermore, these lattice constant values persist in the entire temperature range of the columnar phase, even close to the I-Col coexistence line. Notably, columnar

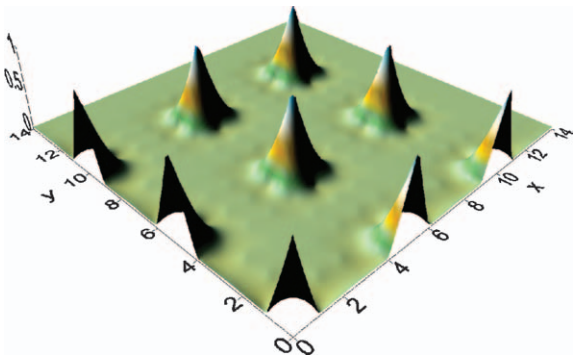

Fig. 4 Calculated two-dimensional density profile, $\rho_\perp(x, y)$, of the fullerene blocks at $p^* = 5$ and $u^* = 0.3$.

phases with unit cells larger than 5×5 are obtained but these solutions correspond to densities within the isotropic–columnar coexistence region of Fig. 3b.

Strictly speaking, the positional organisation of the fullerene–mesogens in the plane perpendicular to the columns is forced to a rectangular columnar ordering due to the imposed cubic lattice restrictions on the positions of submolecular blocks. In other words, the axis parallel to the common orientation of the columns can only be a C4 or a C2 symmetry axis and therefore the only two-dimensional positional order allowed is of rectangular symmetry. This makes it impossible to distinguish between hexagonal and rectangular columnar phases within the present lattice model. However, the phase behaviour of the system, in particular the phase boundaries of the columnar phase to the isotropic or to the smectic phase, is not expected to be severely influenced by this limitation since the free-energy difference between a hexagonal and rectangular columnar phases is expected to be rather low[17] compared to the difference between the columnar (rectangular or hexagonal) and isotropic phase free energy.

3. Monte Carlo simulations

To obtain the exact phase behaviour for the molecular model of the previous section and to gain deeper insight into the molecular organisation, we have executed a series of Monte Carlo (MC) simulations employing the intermolecular potential that we used for the analytical calculations. Working in the constant volume (NVT) ensemble, we place N particles in an orthogonal box that contains $M = N_x N_y N_z$ cubic lattice sites. Standard periodic conditions are applied. A typical run at a given density and temperature consists of approximately 10^6 equilibration MC cycles followed by 10^6 to 10^7 MC production cycles. In a MC cycle each particle makes on average one attempted move.

3.1 Hard particles

In the limit $u^* \to \infty$, the particles behave as impenetrable hard objects and the phase transitions are driven by entropy. The thermodynamically most stable molecular organisation, at a given density, is determined from the balance between translational and orientational entropy. The molecular cones are taken to interact with the potential of eqn (1) but with $u_{\mathrm{f,f}} = u_{\mathrm{f,m}} = u_{\mathrm{m,m}} = \infty$. Constant volume MC simulations ($M = 30 \times 62 \times 28$) were employed for a series of packing fractions $\eta = Nb_n/M$, where

$b_n = 25$ is the number of building blocks per molecule. Starting from a highly ordered tetragonal columnar phase, with packing fraction close to one, we progressively lower the density of the system by removing at random, from the last equilibrated configuration, a number of cones.

The nematic orientational order parameter is defined as $S = \max\{S_{XX}, S_{YY}, S_{ZZ}\}$, where $S_{AA} = \langle 3(\mathbf{z} \times \mathbf{A})^2 - 1\rangle/2$, with the unit vectors **z** and **A** corresponding, respectively, to the principal molecular axis and to any of the macroscopic axes X, Y, Z.

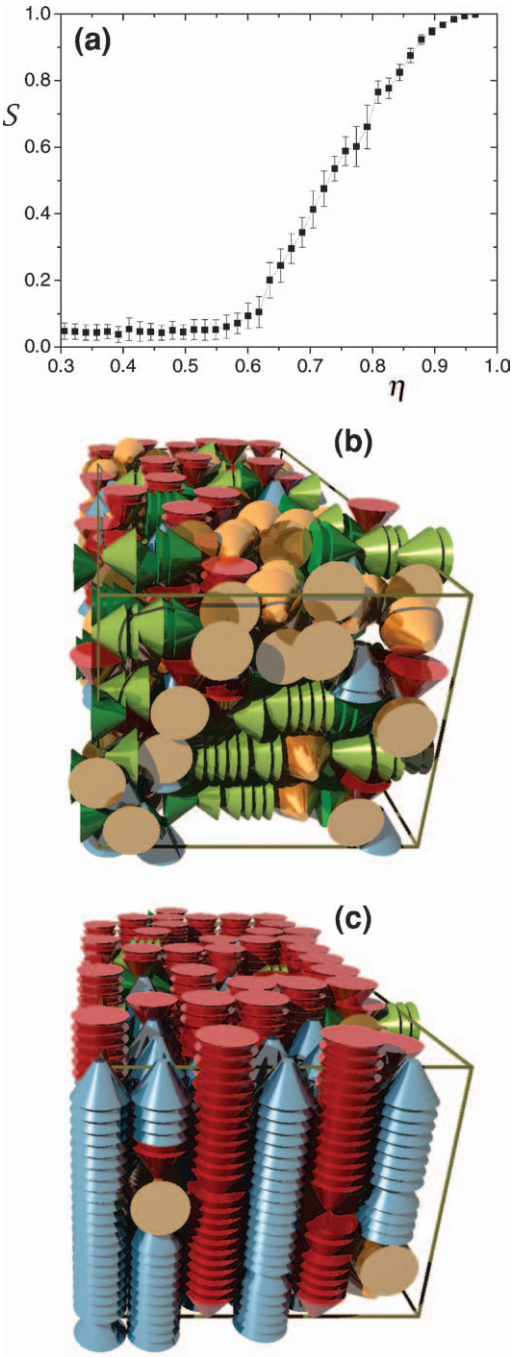

Fig. 5 (a) The orientational order parameter S obtained from the MC simulations as a function of the packing fraction η of the system. (b,c) Typical snapshots for hard cone molecules taken in the isotropic and the columnar phases.

Furthermore, the director, **n**, of the phase is taken to coincide with the axis of the box-frame along which we get the maximum value S. The calculated orientational order parameter is given in Fig. 5a as a function of the packing fraction of the system. Three distinct regions, corresponding to different states of the system, are apparent from this plot. At low densities and up to $\eta = 0.65$ the system is orientationally isotropic. For packing fractions higher than 0.80 the system exhibits high ordering. In the intermediate range, $0.65 < \eta < 0.80$, the orientational order parameter increases nearly linearly with density. Within this range of η, the system is probably in the two-phase (isotropic and columnar) coexistence region. The system appears overall apolar since the polar order parameter $\boldsymbol{P} = \langle \mathbf{z} \rangle$ vanishes in the entire density range. Notably, initial configurations with perfect polar order are found to relax to an apolar columnar phase after sufficiently long runs, even for packing fractions near the maximal value.

Although the orientational order parameter S together with visual inspection of snapshots of the simulated systems (see Fig. 5b and 5c) confirm the columnar organisation of the high density phase, we have calculated a series of pair-correlation functions in order to probe further the molecular organisation of the ordered phase. Taking the macroscopic Z-axis to coincide with the director of the phase, the two-dimensional density profile of the system is obtained through the pair-correlation function

$$f(x, y) = \langle \delta(x - x_{IJ})\delta(y - y_{IJ})\rangle / f^{(id)}(x, y) \quad (3)$$

This gives the probability to find a pair of molecules with the interconnecting vector of their apexes having projections (x, y) in the plane perpendicular to the columns. In eqn (3) $f^{(id)}(x, y)$ is the same probability density for the non-interacting system at the same density. A plot of the above density distribution calculated at $\eta = 0.838$ is given in Fig. 6a, from which it is apparent that a phase is formed having long range two-dimensional positional order with rectangular symmetry and lattice constants $d_x = d_y = 5$. Before terming this phase as liquid crystalline it should be checked whether the system exhibits long-range positional order along the columnar axis. This is achieved by calculating the positional correlations along this axis through the density function

$$f_{\parallel} = \langle \delta(z - z_{IJ})\rangle / f_{\parallel}^{(id)}(z) \quad (4)$$

The calculated $f_{\parallel}(z)$ exhibits only noise fluctuations about a constant value, indicating the absence of long-range positional correlations throughout the studied range of densities.

To quantify the coupled orientational–positional correlations among molecules that belong to the same or different columns, we have calculated the orientation-dependent pair-correlation function $g_\theta(r_\perp)$ defined as

$$g_\theta(r_\perp) = \langle \delta(r - r_{\perp;IJ})\cos\theta_{IJ}\rangle / \langle \delta(r - r_{\perp;IJ})\rangle \quad (5)$$

where $r_{\perp;IJ} = \sqrt{\mathbf{r}_{IJ}^2 - (\mathbf{r}_{IJ}\mathbf{n})^2}$ and $\cos\theta_{IJ} = \mathbf{z}_I \times \mathbf{z}_J$. In Fig. 6b we plot the calculated function $g_\theta(r_\perp)$ at $\eta = 0.838$. The value of $g_\theta(r_\perp)$ at $r_\perp = 0$ gives the intracolumnar orientational correlations. Clearly each column is highly polar with nearly 86% of the cones pointing in the same direction but the phase is overall apolar, in accord with the analytical results. Notably, the intercolumnar polar

This journal is © The Royal Society of Chemistry 2008

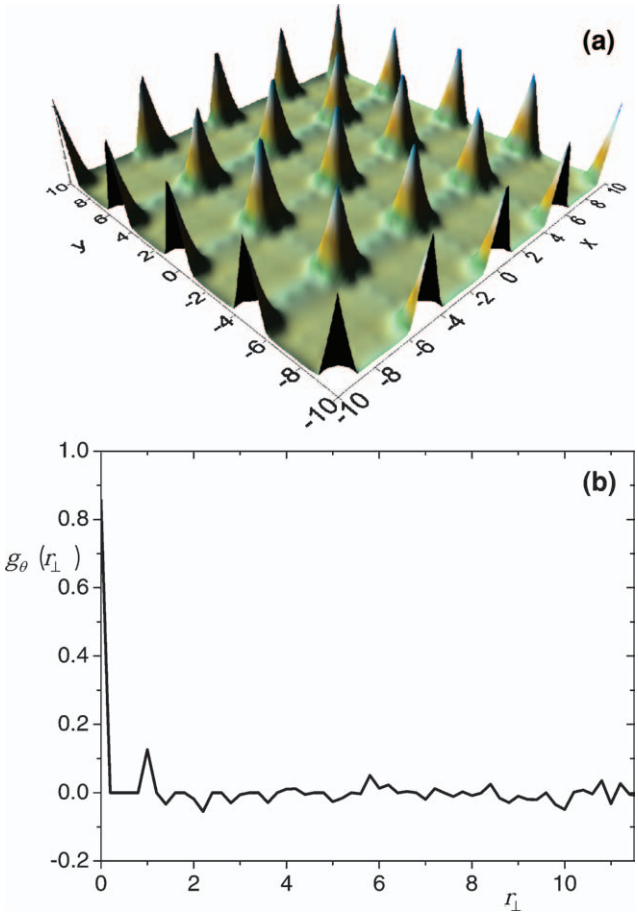

Fig. 6 Plots of (a) the simulated density function $f(x, y)$ of eqn (3) showing the positional correlations of the fullerene units for hard cones and (b) the simulated orientational correlation function $g_\theta\ (r_\perp)$ of eqn (5) for hard cones at $\eta = 0.838$.

orientational correlations are seen in Fig. 6(b) to vanish already at first neighbour distances, indicating the absence of polar domains beyond a single column.

Despite the fact that theory overestimates both, the transition pressure and the density jump at the transition, a known drawback of the Onsager-type free-energy functionals, the results of the simulations confirm the basic theoretical predictions according to which 1) in the limit of hard interactions only two liquid phases, an isotropic and a liquid-crystal columnar, are involved in the phase sequence of the system 2) columns are formed by directional molecular stacking, therefore exhibiting high polarity and 3) the columnar phase, although composed of polar columns, is overall apolar.

3.2 Soft cones with hard apex

To study how the softness of the conical periphery influences the phase behavior of the system we have run a set of constant volume simulations where we vary gradually the interaction parameter u^*. The density range was chosen so as to yield thermodynamically stable columnar phases at high values of the interaction parameter u^* (equivalently, at low temperatures). Thus, guided by the results of the previous section for hard cones, we focused our calculations on systems with $\eta > 0.8$.

Here we present results for a system at density $\eta = 0.8295$ to which we have applied both, cooling and heating sequences. The simulation box contains $M = 30 \times 62 \times 28$ cubic lattice sites; at the specified density this corresponds to $N = 1728$ molecules. In a cooling run we start from a high temperature and a well

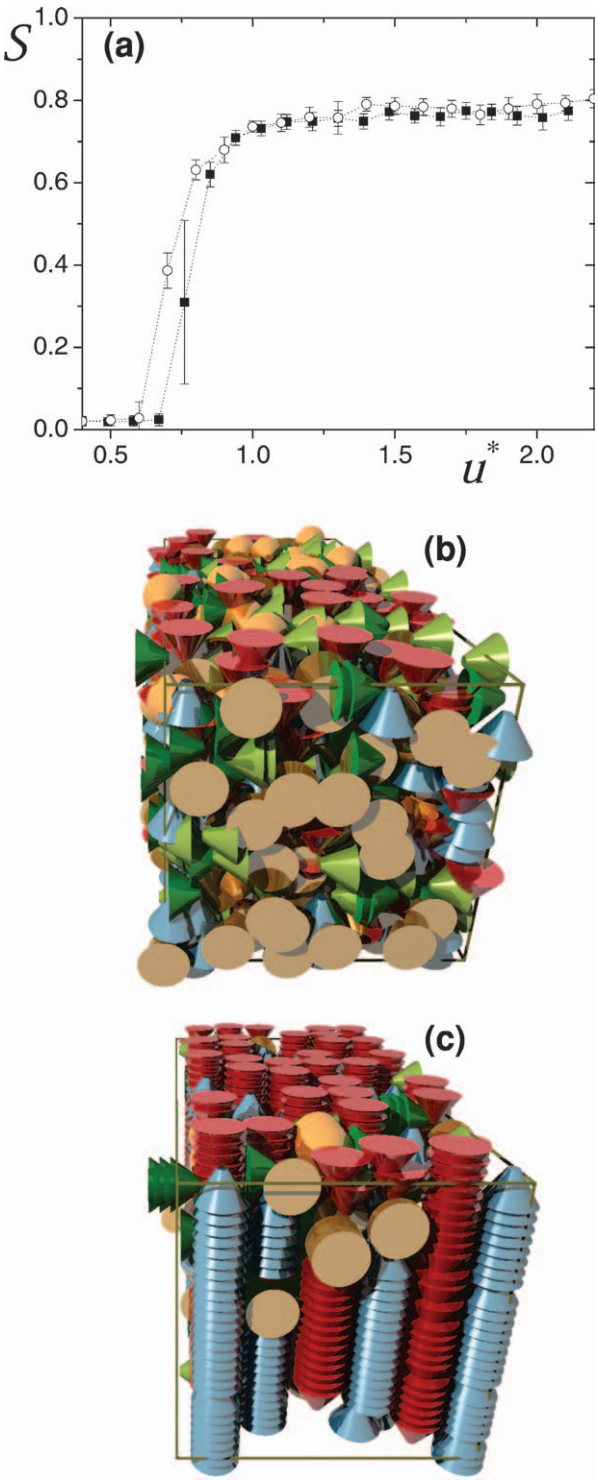

Fig. 7 (a) Plot of the simulated orientational order parameter S as a function of the interaction parameter u^* (cooling: squares, heating: open circles). (b,c) Typical snapshots for soft cone molecules corresponding to the isotropic and columnar phases.

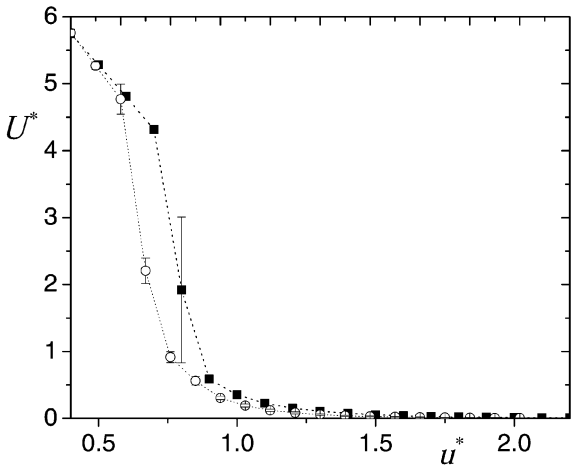

Fig. 8 Calculated mean potential energy per particle, in units of the interaction strength u, as a function of the interaction parameter u^* (cooling: squares, heating: open circles).

equilibrated isotropic state of the system and decrease the temperature gradually. In heating runs, we start from a perfectly ordered state and increase the temperature in small steps. In both cases, the final equilibrated configuration of the system for each temperature is used as the starting configuration for the next simulated temperature.

In Fig. 7a we present the evolution of the orientational order parameter S as a function of the interaction parameter u^*, obtained for cooling and heating runs. Obviously the system exhibits a sharp order–disorder phase transition at $u^* \approx 0.8$. Snapshots of the simulated phases at high temperatures (low interaction parameter) and at low temperatures (high interaction parameter) reveal, respectively, the isotropic and the columnar organization of the system (Fig. 7b and 7c). Furthermore, the small observed hysteresis is indicative of the first-order nature of the transition. The analysis of the molecular organisation in terms of the pair-correlation functions, introduced in the previous section through eqn (3)–(5), leads to similar conclusions concerning the molecular organisation in the columnar phase: the phase is overall apolar, consisting of highly polar columns that slide one beside the other, thus preventing the development of appreciable long-range positional correlations along the column axes.

In contrast to the case of hard body interactions, the softness of the conical periphery allows for intermolecular overlaps (two addend blocks belonging to different molecules may occupy the same space). As a measure of the mutual overlap, we have calculated $U^* \equiv \langle U/u \rangle / N$, *i.e.* the average potential energy per particle in units of the interaction strength u. The results are plotted in Fig. 8, from which it becomes apparent that, at high temperatures in the isotropic phase, more than four molecular blocks on average share the same space with addend blocks of other molecules while in the columnar phase this number vanishes, indicating the absence of molecular overlapping.

4. Conclusions

We have used a simplified molecular model of cubic building blocks to describe the mesomorphism of conical fullerenomesogens. As the same type of block model has been applied successfully to fulleromesogens of various other architectures,[22] the present study constitutes a further test of this model, this time against the experimentally observed[19,20,23] mesomorphic behaviour of fullerene "badminton shuttlecocks".

Applying Onsager-type density functional theory and MC computer simulations, we studied the phase behaviour of the block–model conical fulleromesogens. Both, analytical calculations and computer simulations, give qualitatively similar results that are also in good agreement with the experimentally observed phase sequences.

Theory and computer simulations indicate that the formation of thermodynamically stable columnar mesophases of conical fulleromesogens is entropically driven, although molecular polyphilicity plays a synergetic role in the stabilisation of the columnar phase over the isotropic. For fixed geometrical characteristics of the molecular cone shape, a single model parameter, combining temperature with softness of the repulsive interactions among molecular segments, is found to control the order–disorder phase transitions as well as the relative thermodynamic stability of the lamellar over the columnar molecular ordering.

Despite the strongly polar shape of the molecules and the strongly polar local ordering identified in both the theoretical calculations and the molecular simulations, the stable mesophases are found in all cases to be macroscopically apolar.

Acknowledgements

SDP acknowledges funding from the European Social Fund (ESF), Operational Program for Educational and Vocational Training II (EPEAEK II) through the Program IRAKLEITOS.

References

1 S. Chandrasekar, in *Advances in Liquid Crystals*, ed. G. H. Brown, Academic Press, New York, vol. 5, 1982; D. Demus, J. W. Goodby, G. W. Gray, H. W. Spiess and V. Vill (editors), Handbook of Liquid Crystals: Low Molecular Weight Liquid Crystals II: Discotic and Non-Conventional Liquid Crystals, Wiley-VCH, New York, 1998, and references therein.
2 S. Chandrasekhar, B. K. Sadashiva and K. A. Suresh, *Pramana*, 1977, **9**, 471.
3 K. E. S. Phillips, T. J. Katz, S. Jockusch, A. J. Lovinger and N. J. Turro, *J. Am. Chem. Soc.*, 2001, **123**, 11899.
4 S. Hoger, V. Enkelmann, K. Bonrad and C. Tschierske, *Angew. Chem., Int. Ed.*, 2000, **39**, 2268.
5 K. Kanie, M. Nishii, T. Yasuda, T. Taki, S. Ujiie and T. Kato, *J. Mater. Chem.*, 2001, **11**, 2875.
6 K. Kishikawa, S. Furusawa, T. Yamaki, S. Kohmoto, M. Yamamoto and K. Yamaguchi, *J. Am. Chem. Soc.*, 2002, **124**, 1597.
7 F. Morale, R. W. Date, D. Guillon, D. W. Bruce, R. L. Finn, C. Wilson, A. J. Blake, M. Schroder and B. Donnio, *Chem.–Eur. J.*, 2003, **9**, 2484.
8 A. J. Paraskos, Y. Nishiyama and T. M. Swager, *Mol. Cryst. Liq. Cryst.*, 2004, **411**, 1405.
9 Lin Lei, *Wuli*, 1982, **11**, 171; J. Malthete and A. Collet, *J. Am. Chem. Soc.*, 1987, **109**, 7544.
10 H. Zimmennann, R. Poupko, Z. Luz and J. Billard, *Z. Naturforsch.*, 1985, **40**, 149.
11 A. M. Levelut, J. Malthete and A. Collet, *J. Phys. (Paris)*, 1986, **47**, 351.
12 H.-T. Jung, S. O. Kim, Y. K. Ko, D. K. Yoon, S. D. Hudson, V. Percec, M. N. Holerca, W.-D. Cho and P. E. Mosier, *Macromolecules*, 2002, **35**, 3717.
13 J. Lenoble, N. Maringa, S. Campidelli, B. Donnio, D. Guillon and R. Deschenaux, *Org. Lett.*, 2006, **8**, 1851.
14 K. Rais, M. Daoud, M. Gharbia, A. Gharbi and H. T. Nguyen, *ChemPhysChem*, 2001, **2**, 45.

 This journal is © The Royal Society of Chemistry 2008

15 H. Shen, K.-Un Jeong, H. Xiong, M. J. Graham, S. Leng, J. X. Zheng, H. Huang, M. Guo, F. W. Harris and S. Z. D. Cheng, *Soft Matter*, 2006, **2**, 232.
16 B. Donnio, B. Heinrich, H. Allouchi, J. Kain, S. Diele, D. Guillon and D. W. Bruce, *J. Am. Chem. Soc.*, 2004, **126**, 15258; E. Gorecka, D. Pociecha, J. Mieczkowski, J. Matraszek, D. Guillon and B. Donnio, *J. Am. Chem. Soc.*, 2004, **126**, 15946.
17 P. K. Karahaliou, P. H. J. Kouwer, T. Meyer, G. H. Mehl and D. J. Photinos, *Soft Matter*, 2007, **3**, 857.
18 C. Tschierske, *Nature*, 2002, **419**, 681.
19 M. Sawamura, K. Kawai, Y. Matsuo, K. Kanie, T. Kato and E. Nakamura, *Nature*, 2002, **419**, 702.
20 Y. Matsuo, A. Muramatsu, R. Hamasaki, N. Mizoshita, T. Kato and E. Nakamura, *J. Am. Chem. Soc.*, 2004, **126**, 432.
21 A. G. Vanakaras and D. J. Photinos, *Mol. Cryst. Liq. Cryst.*, 2003, **395**, 213.
22 S. D. Peroukidis, A. G. Vanakaras and D. J. Photinos, *J. Chem. Phys.*, 2005, **123**, 164904; A. G. Vanakaras and D. J. Photinos, *J. Mater. Chem.*, 2005, **15**, 2002.
23 Yu-Wu Zhong, Y. Matsuo and E. Nakamura, *J. Am. Chem. Soc.*, 2007, **129**, 3052.

This journal is © The Royal Society of Chemistry 2008